CrossMark

Design of dual-polarized triple-band concentric annular-ring microstrip patch antenna for GPS applications

Surya Deo Choudhary[1] , Shilpee Patil[1] , Alka Verma[2] , Md Irshad Alam[3],
Vinod M. Kapse[1] and Binod Kumar Kanaujia[4]

[1]Department of Electronics and Communication Engineering, Noida Institute of Engineering and Technology, Greater Noida, Uttar Pradesh, India; [2]Electronics Engineering, A.K.T.U, Lucknow, Uttar Pradesh, India; [3]Department of Electrical Engineering, Sitamarhi Institute of Technology, Sitamarhi, Bihar, India and [4]School of Computational and Integrative Sciences, Jawaharlal Nehru University, New Delhi, India

Abstract

A triple-frequency operated concentric annular ring microstrip antenna which is single fed is presented. The proposed antenna with three concentric annular rings and two symmetrical notches on its outer ring and having a cross slot in its ground surface shows triple band at resonance frequency 1.22760, 1.57542, and 2.18 GHz, respectively. At the first two bands (GPS L2 and GPS L1), circular polarization characteristic is observed and the third band observes linear polarization finding its application in Universal Mobile Telecommunication System (UMTS). The complete dimension of the antenna designed and fabricated is only $51.6 \times 51.6 \times 1.6 \text{ mm}^3$. Experimental results depict the proposed antenna gain of 3.31, 3.55, and 3.50 dBi in three bands, respectively, and closely matches with the theoretical results.

Introduction

In the present scenario, circularly polarized (CP) antennas have widely gained attention finding their application in various wireless systems such as Satellite Communication, Global Positioning System (GPS), etc. Compactness followed by multiband operation of CP antenna has been an inspiration for various researchers in wireless communication systems. Various antennas such as slot antenna [1–5], fractal antenna [6–8], monopole antenna [9, 10] have been extensively designed to obtain multiband. The use of annular ring antennas [11–13] has also become a very promising applicant for multiband applications because of their simple structure and design flexibility in obtaining miniaturization. For generation of CP waves, many techniques were adopted by researchers which included the perturbation method [14, 15], slots [16, 17], slits [18], metamaterial [19–21], stacking [22,23], etc. Using the above techniques, many designs have been reported by various researchers to obtain triple-band [24, 25] and dual-band [26, 27] CP antennas. In [28] by using quadrature feeding, an F antenna was designed and was able to generate right-hand circularly polarized (RHCP) waves in all the three GPS bands *L*1, *L*2, and *L*5 but led to poor gain in the *L*1 band due to the air gap in the stacking of two substrates. In [29] dual-band circular patch antenna with two concentric annular rings with slot-loaded ground plane was designed to achieve dual-band CP but it suffered from poor front-to-back ratio due to diffraction from the slots in the ground plane. In [30] a dual-band CP antenna is discussed for GPS *L*5 and SDARS bands. In [31] a dual-band CP antenna having concentric annular rings and fed by four apertures was designed to obtain RHCP waves in the two bands. The above design lacked simplicity as phase shifters and Wilkinson power combiners were implemented to produce the required circular polarization. In [32] a cavity-backed annular slot antenna was designed with a dimension of $80 \times 80 \text{ mm}^2$ dual-band *L*1 and *L*2, and CP is achieved with low gain in the two bands. In [33] the GPS antenna is proposed by modifying an annular ring and the SDARS antenna is placed at the ring center using a slot-loaded degenerate mode square patch. In [34] a Y-shaped monopole antenna was designed which achieved triple band at 2.4, 3.5, and 5.8 GHz and with dual-polarization at the first and third band but <2.5 dBi gain in all the bands. In [35], a triple-band CP antenna was designed by stacking a truncated square microstrip antenna with an ellipse-shaped microstrip antenna. The above antenna showed CP characteristics at the first two bands 4.2 and 4.8 GHz with linear polarization characteristic in the third band of 5.8 GHz, but the stacking process led to a lack of compactness in size. Thus, the literature survey led to the conclusion that to obtain multiband antenna generating CP waves along with the performance of antenna in terms of gain, impedance bandwidth, AR bandwidth improving and achieving miniaturization of the antenna is a challenging task.
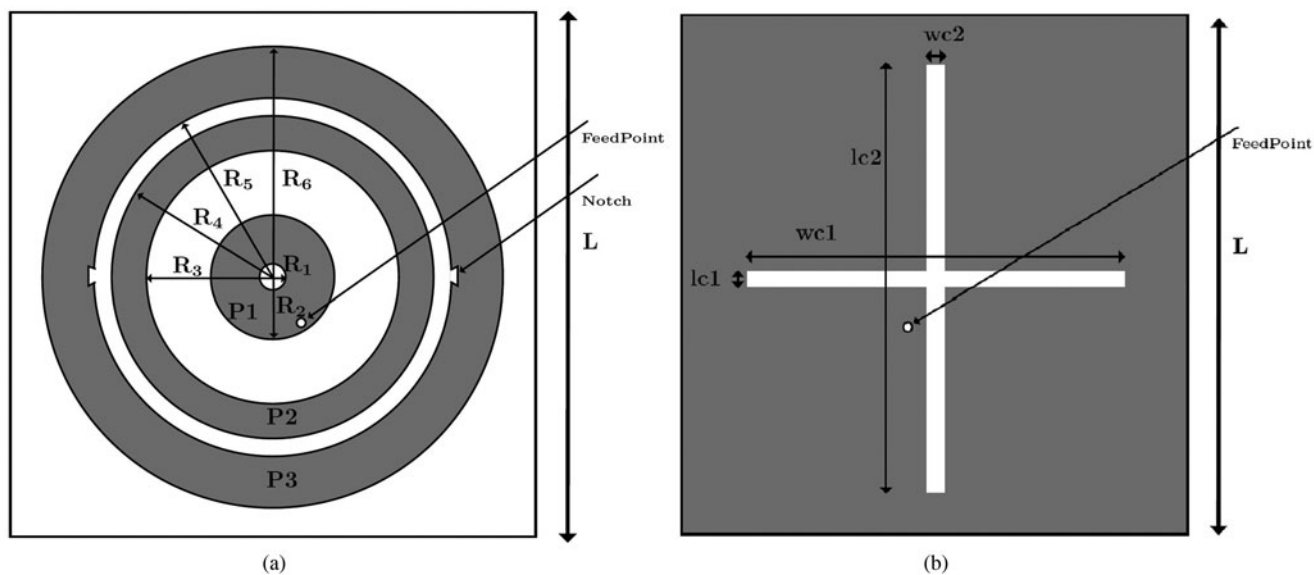
CAMBRIDGE
UNIVERSITY PRESS

Fig. 1. Geometry of proposed antenna. (a) Top view. (b) Bottom view.

Table 1. Parameters of the proposed antenna

Parameters	R1	R2	R3	R4	R5	R6
Value (mm)	0.99	5.74	11.28	14.88	16.88	22.40
Parameters	L	lc1	wc1	lc2	wc2	h
Value (mm)	51.6	0.86	34.57	36.65	1.34	1.6

In this article, with the aim of achieving compactness followed by achieving multiband and observing CP characteristic, a novel triple-band dual-polarized annular ring antenna is proposed. In this design by implementing two layers of concentric ring around an annular ring leads to the generation of three bands showing circular polarization in the first two bands and linear polarization in the third band. A detailed theoretical approach is presented by the approach of the equivalent circuit and the simulation analysis is done using CST Microwave Studio matching well the measured results. The proposed antenna has an attractive feature of being simple with a low profile for achieving the desired frequency of $L2$ and $L1$ bands and thus making the above structure finding its application for GPS with RHCP in the two bands having 3 dB beamwidth of 107.70 and 119.32° respectively.

Design and theoretical analysis

Figure 1 shows concentric annular ring microstrip antenna (CARMSA). The inner annular ring patch antenna ($P1$) is coaxially fed whereas the other two concentric rings ($P2$ and $P3$) surround the patch. The outermost concentric annular ring $P3$ is having two notches placed symmetrically on it to get the desired resonating frequency and improved axial ratio. The proposed structure is built on FR4 substrate (relative permittivity 4.4) of height 1.6 mm. The ground plane of $L \times L$ is embedded with a cross slot of $lc1 \times wc1$ and $lc2 \times wc2$. To get the desired resonant frequency, the two notches are etched inside the outermost concentric annular ring. The vertex of symmetrical notches is at

(16.82, 0.75), (16.82, −0.75), (17.43, −1), and (17.43, 1) in mm. Table 1 shows the dimensional parameters of the proposed antenna.

DGS unit can be modeled as parallel R, L, and C resonant circuit as in Fig. 2(a), which is connected at both ends to transmission lines [36].

The concentric annular ring microstrip patch can be represented by an equivalent circuit as shown in Fig. 2(b). This circuit includes a parallel combination of resistance $R1$, inductance $L1$, and capacitance $C1$, which represent the unit cell of annular ring patch $P1$. Annular ring $P2$ is represented as a parallel combination of resistance $R2$, inductance $L2$, and capacitance $C2$. Rings $P1$ and $P2$ are coupled with a parallel plate capacitance ($Cs1$) and two fringing capacitances ($Cp1$). Similarly, the outer most ring $P3$ (parallel combination of $R3$, $L3$, and $C3$) is coupled with $P1$ and $P2$ by a parallel plate capacitance ($Cs2$) and two fringing capacitances ($Cp2$) [37]. A coupling capacitance ($Cs3$) is considered between the slot integrated ring and without the slot integrated ring which is connected in series with parallel combination of Rn, Ln, and Cn. Coaxial feed is represented by series combination of resistance Rf and inductance Lf as shown in Fig. 2(a).

The total input impedance of the equivalent circuit (Z_{eq}) can be expressed as [38]:

$$Z_{eq} = Rf + j\omega Lf + \frac{Zn(Zp + (1/j\omega Cs3))}{(Zp + Zn + (1/j\omega Cs3))} ,$$

where $Zn = (1/Rn + j\omega Ln + (1/j\omega Cn))$ is the input impedance of symmetrical notches.
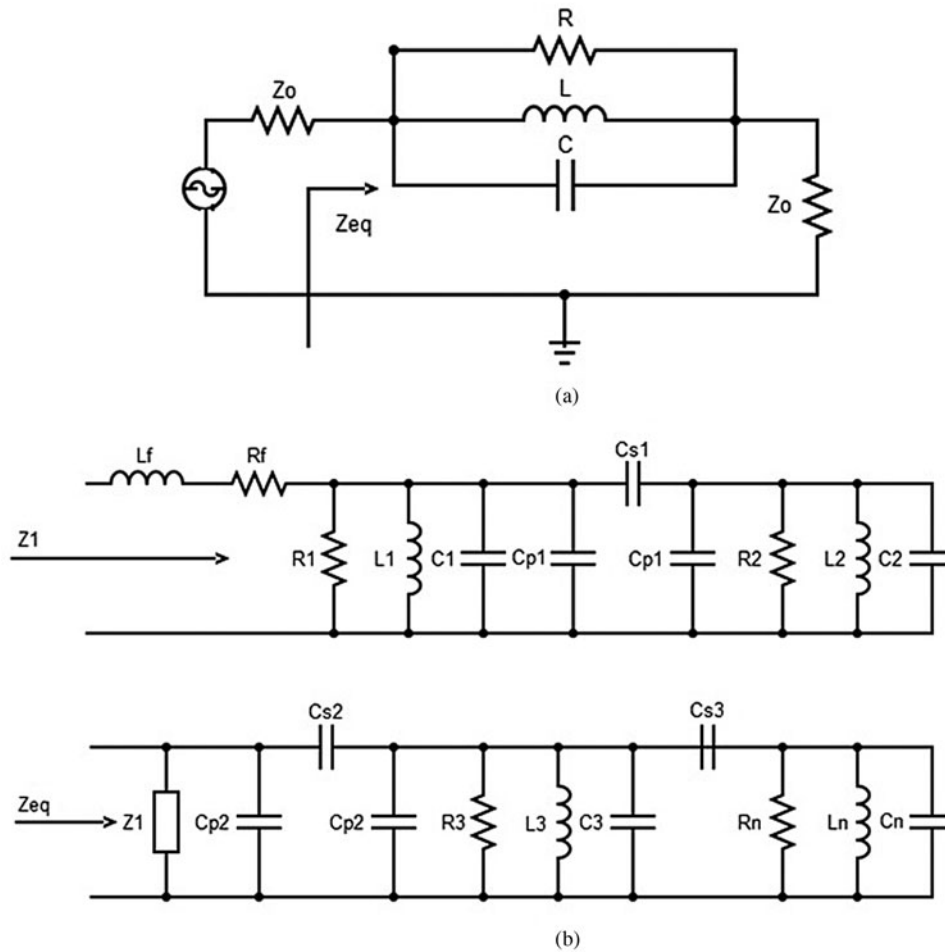
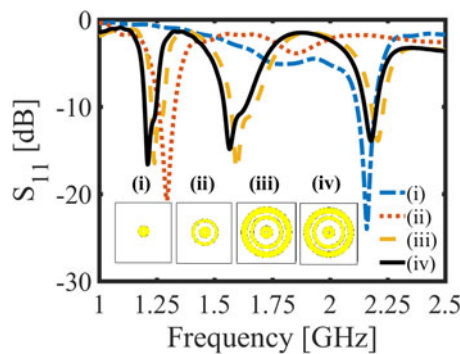Fig. 2. Equivalent circuit model of (a) cross slot and (b) proposed CARMSA.

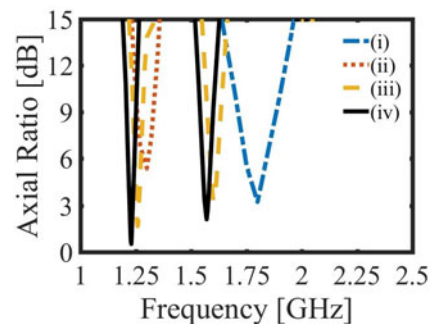Fig. 3. Variation of simulated S_{11} with frequency of evolution of antennas.

Fig. 4. Variation of axial ratio with frequency of evolution of antennas.

Z_p = equivalent impedance of coupled $P1$, $P2$, and $P3$.

Components of the equivalent circuit $R1$, $L1$, and $C1$ can be expressed as [38]:

$$L1 = \frac{\varepsilon_n^2 \mu_0 h}{\pi k^2} \frac{\{F(d)\}^2}{[b^2(1-(n^2/k^2 b^2))\{F(b)\}^2 - a^2(1-(n^2/k^2 b^2))\{F(a)\}^2]},$$

where $F(b) = (j_n(kb)y_n'(ka) - y_n(ka)j_n'(kb))$,

where a is the inner radius and b the outer radius of annular ring, ε_r is the relative permittivity of the substrate, ϵ_0 is the free space permittivity, d is the feed point, k is the resonant wave number, h is the thickness of the substrate, μ_0 is the permeability of free space, $\varepsilon_n = \sqrt{2}$ (for $n \neq 0$), $\varepsilon_n = 1$ (for $n = 0$).

$$C1 = \frac{\varepsilon_0 \varepsilon_r \pi}{\varepsilon_n^2 h} \frac{[b^2(1-(n^2/k^2 b^2))\{F(b)\}^2 - a^2(1-(n^2/k^2 b^2))\{F(a)\}^2]}{\{F(d)\}^2},$$
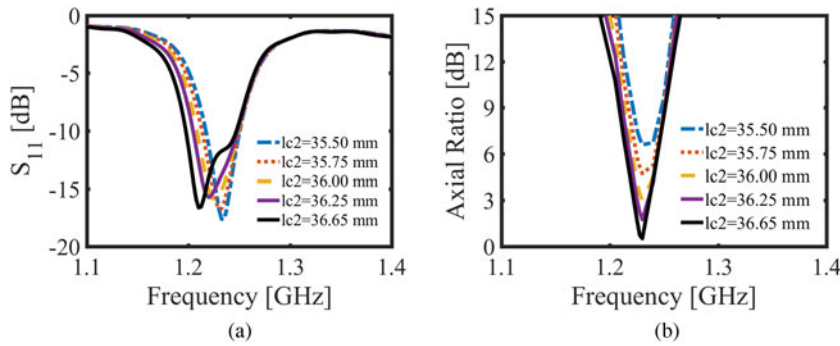
$$R1 = \frac{Q_0}{\pi f C1},$$

Fig. 5. (a) Influence of length $lc2$ on S_{11} versus frequency. (b) Influence of length $lc2$ on axial ratio versus frequency.
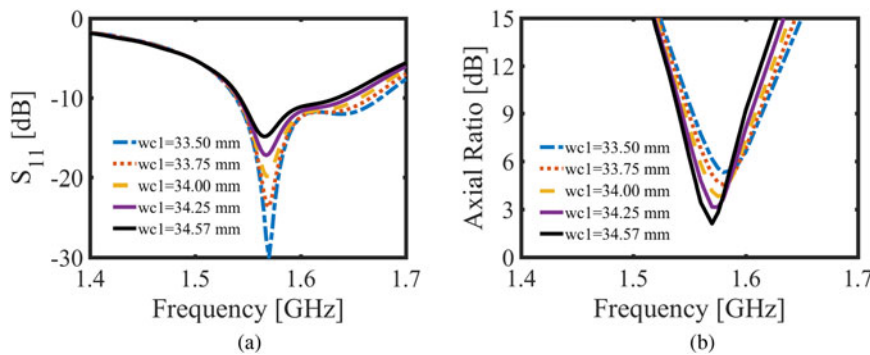

Fig. 6. (a) Influence of length $wc1$ on S_{11} versus frequency. (b) Influence of length $wc1$ on axial ratio versus frequency.

where Q_0 is a factor including radiation, conductor, and dielectric losses.

Evolution stages of the proposed antenna

The evolution of our proposed antenna started with a coaxial fed annular ring antenna (i) of inner radius $R1$ and outer radius $R2$. The ground plane of the antenna was loaded with cross slot. As seen in the figure, this proposed antenna resonates at 2.16 GHz and achieves a bandwidth of 78.279 MHz (2.1183–2.1966 GHz) with linear polarization at 2.16 GHz. A concentric ring of inner radius $R3$ and outer radius $R4$ is made to surround the antenna (i) to shift the resonant frequency of the antenna to the lower side of 1.295 GHz. As depicted in Fig. 3, the impedance bandwidth achieved is 71.12 MHz (1.2572–1.3283 GHz). The axial ratio of 5.62 dB at 1.295 GHz is obtained. To get triple band, a second concentric annular ring of inner radius $R5$ and outer radius $R6$ is introduced which generates three bands at 1.22760, 1.57542, and 2.18 GHz of impedance bandwidth 54.032, 105.43, and 52.057 MHz, respectively. Figure 4 depicts that CP waves are also generated at 1.22760 GHz having an AR bandwidth of 12 MHz (1.222–1.234 GHz) with LP waves generated at 1.57542 and 2.18 GHz. A notch is introduced in the second concentric ring, and it is observed that the resonant frequency shifts to desired three bands being generated at 1.22760, 1.57542, and 2.18 GHz. It is also observed from this figure, dual CP band is at 1.22760 and 1.57542 GHz with AR bandwidth of 14.30 MHz (1.2221–1.2364 GHz) and 13.60 MHz (1.5630–1.5766 GHz), respectively. The axial ratio of 0.73 dB at 1.22760 GHz and 2.81 dB at 1.57542 GHz is obtained.

Parametric study of proposed antenna

To get the desired frequency band, a parametric analysis was carried on the proposed antenna by varying the dimensions of the
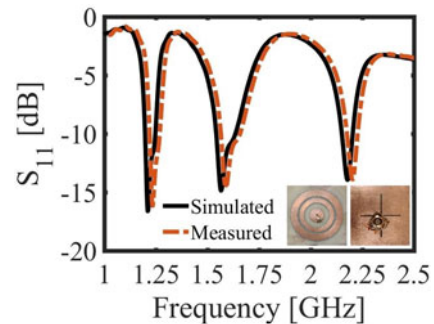

Fig. 7. Simulated and measured S_{11} of proposed antenna.

cross slot in the ground plane and their effect on S_{11} and axial ratio with frequency was studied.

Influence of length lc2

Variation of $lc2$ on the S_{11} and axial ratio with frequency is observed in Figs 5(a) and 5(b). As $lc2$ is considered at 35.50, 35.75, 36, 36.25, and 36.65 mm, it is observed that the resonant frequency of the proposed antenna is achieved at 1.2350, 1.2325, 1.2310, 1.2295, and 1.22760 GHz, respectively. Thus, it is observed that as length increases from 35.50 to 36.65 mm, resonating frequency shifts toward lower frequency to achieve GPS $L2$ band at resonating frequency of 1.22760 GHz. From Fig. 5 (b) it is also observed that axial ratio improves at 36.65 mm with axial ratio value approaching the ideal value of 0.73 dB from 5.62 dB as length increases. Thus, the value of $lc2$ is set to 36.65 mm.
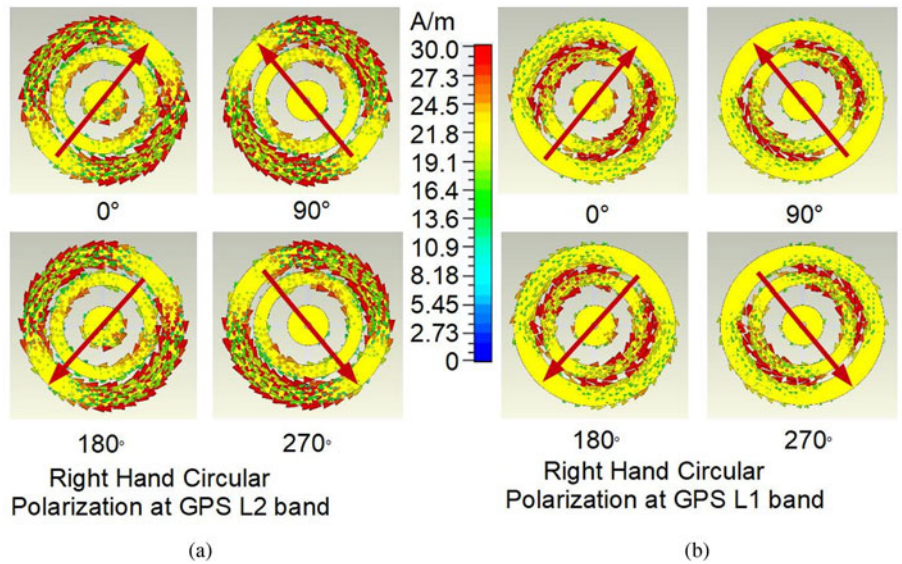
Fig. 8. Surface current distribution at 1.22760 and 1.57542 GHz for the signal excitation at $t = 0$, that is, 0° phase, $t = T1/4$, that is, 90° phase, $t = T1/2$, that is, 180° phase and $t = 3T1/4$, that is, 270°.
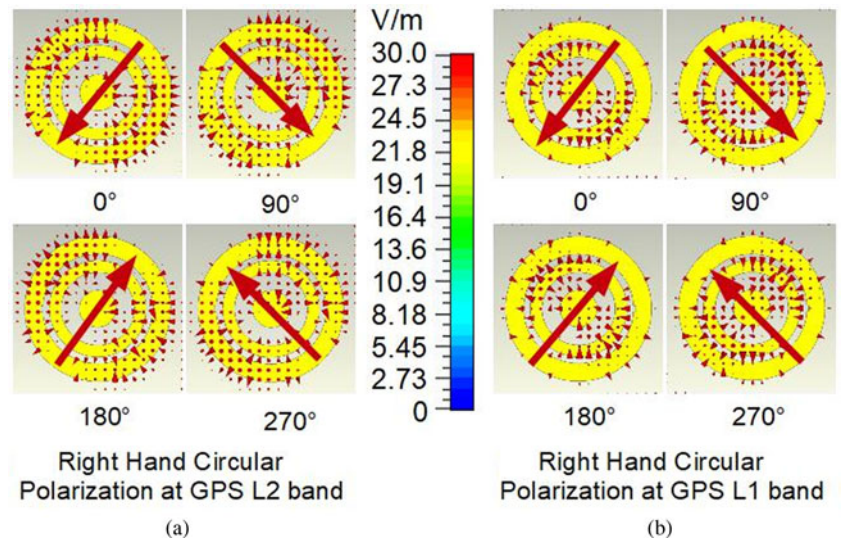
Fig. 9. Electric field distribution at 1.22760 and 1.57542 GHz for the signal excitation at $t = 0$, that is, 0° phase, $t = T1/4$, that is, 90° phase, $t = T1/2$, that is, 180° phase and $t = 3T1/4$, that is, 270°.
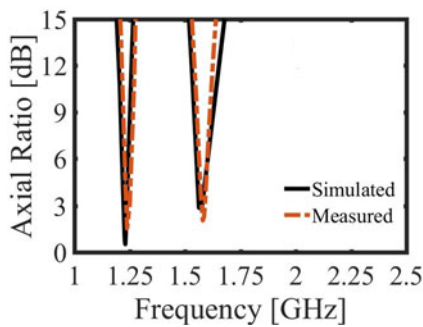
Fig. 10. Simulated and measured axial ratio of proposed antenna.
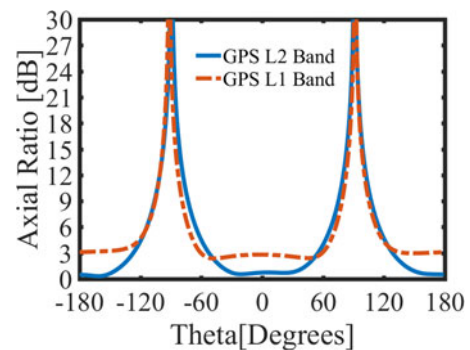
Fig. 11. Axial ratio of the designed antenna exhibits wider beamwidth.

Influence of length wc1

Variation of *wc*1 on the S_{11} and axial ratio with frequency is observed in Figs 6(a) and 6(b). As *wc*1 is considered at 33.50, 33.75, 34, 34.25, and 34.57 mm, the value of S_{11} shifts toward upper frequency to achieve GPS *L*1 band at resonating frequency 1.57542 GHz and better impedance matching is observed at 34.57 mm. It is also observed
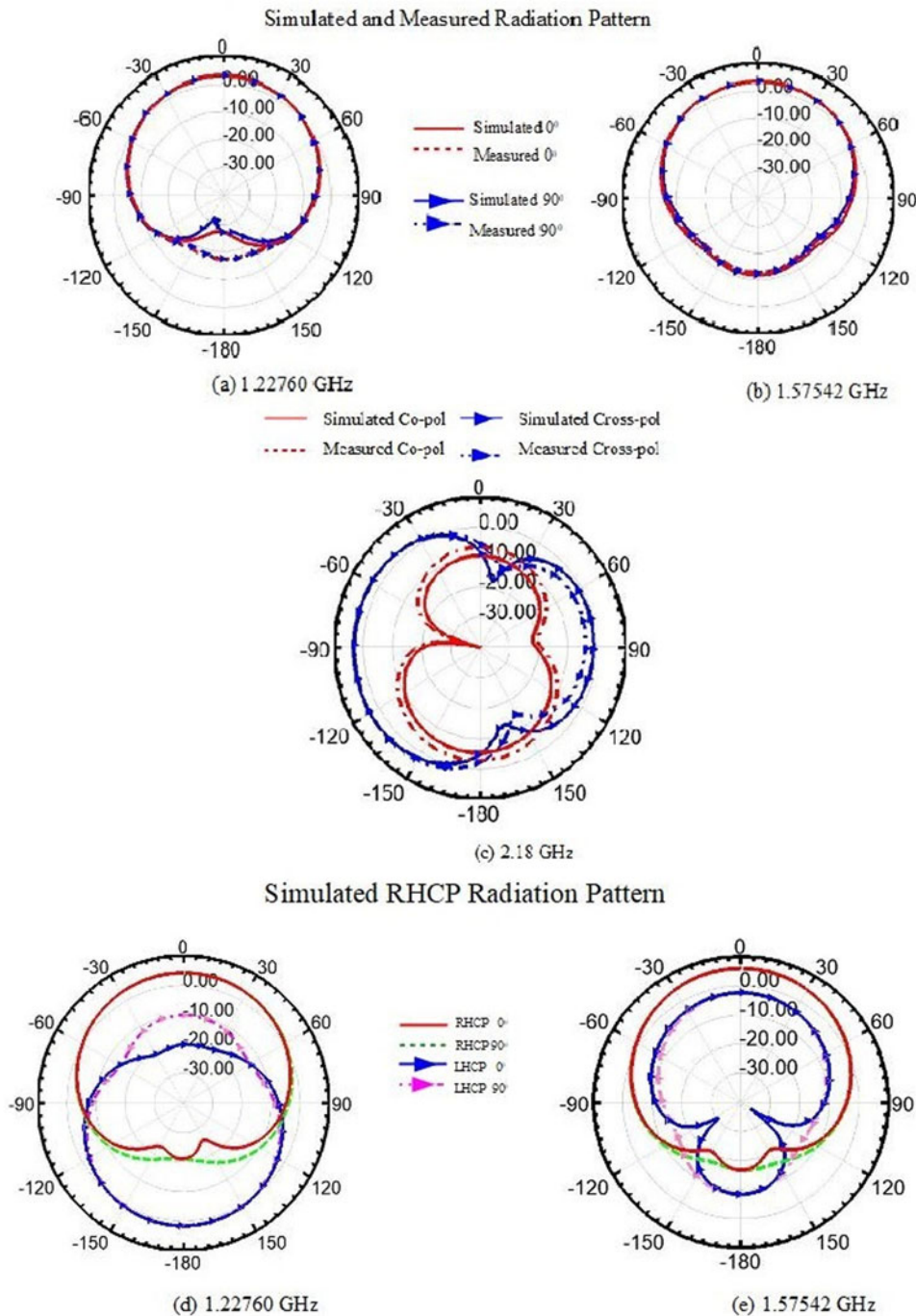
Fig. 12. Radiation pattern of proposed antenna at GPS *L*2, GPS *L*1, and UMTS bands.

that axial ratio improves at 34.57 mm with axial ratio value approaching the ideal value of 2.81 dB at desired frequency 1.57542 GHz from 5.56 dB as the value of *wc*1 increases from 33.50 to 34.57 mm. Thus, the value of *wc*1 is finalized to 34.57 mm.

Results and discussion

By using the Agilent vector analyzer (N5230A: PNA-L), the fabricated model of the proposed antenna is obtained. Figure 7 depicts the top and bottom view of the fabricated prototype of the proposed antenna. Figures 8 and 9 show the vector surface current and electric

field distribution that are analyzed by varying the time phase at 0, 90, 180, 270° at 1.22760 and 1.57542 GHz, respectively. At 0 and 90°, the vector surface current and electric field are of the equal magnitude and are in-phase opposition at 180 and 270°, respectively. This concludes that as there is change in the phase, and the simulated surface current vectors and electric field rotate in the anticlockwise direction, demonstrating that RHCP is achieved.

Figures 7 and 10 depict that the proposed antenna achieves measured impedance bandwidth of 49.50 MHz (1.1994–1.2489 GHz), 94.10 MHz (1.5444–1.6385 GHz), and 52.60 MHz (2.1550–2.2076 GHz) and AR bandwidth of 15.50 MHz

Table 2. Comparison of our proposed antenna with some reported CP antennas in the literature

Ref.	Size (mm³)	Dielectric constant	Resonating freq. (GHz)	Impedance bandwidth (MHz)	3 dB Axial ratio bandwidth (MHz)	Gain (dBic)	Beamwidth (degree)
[28]	38 × 38 × 20	25	1.17	24	–	2	110
		12	1.22	24		2	90
			1.57	24		0	
[29]	60 × 60 × 1.52	4.0	1.22	72	12	1.35	–
			1.48	90	16	3.5	–
[30]	65 × 65 × 1.6	4.4	1.17645	48	13	4.2	116
			2.3325	51	25	6.6	120
[31]	53 × 53 × 5	4.5	–	–	75	5	110
					58		110
[32]	80 × 80 × 1.6	4.4	1.21	40	11	2.95	–
			1.57	20	9	1.5	
[33]	116 × 116 × 3.7	–	1.57542	20	–	7.2	–
			2.3325	35		6.5	
[34]	35 × 45 × 1.6	4.4	2.4	230	110	<3	–
			3.5	170	–		
			5.8	4170	400		
[35]	30 × 30 × 1.52	2.2	4.2	–	–	7	–
			4.8			–	
			5.8			–	
Proposed antenna	51.6 × 51.6 × 1.6	4.4	1.22760	49.50	15.50	3.32	107.70
			1.57542	94.10	14.20	3.54	119.32
			2.18	52.60	–	3.83	–

(1.2239–1.2394 GHz) and 14.20 MHz (1.5651–1.5793 GHz) which has good agreement with simulated ones. These results satisfy the desired frequency of GPS *L*2, GPS *L*1, and UMTS bands. Figure 11 depicts the simulated axial ratio beamwidth of 107.70 and 119.32° for GPS *L*2 and GPS *L*1 bands.

The gain of the proposed antenna varying with frequency is illustrated in Fig. 12. It is observed from radiation patterns that the simulated gain attains the value of 3.32 dBic in the first band, 3.54 dBic in the second band, and 3.83 dBic in the third band. The simulated results match closely with the measured gain of 3.31, 3.55, and 3.5 dBic in the three bands. This figure shows the radiation pattern at 1.22760, 1.57542, and 2.18 GHz for E and H planes.

Figures 12(d) and 12(e) depict the radiation pattern for simulated RHCP of the proposed antenna for both GPS *L*2 and GPS *L*1 frequency bands. Observation shows that the pattern is symmetrical for GPS *L*2 band and its RHCP is greater than left-hand CP by 27 dB and for GPS *L*1 band RHCP is greater than left-hand CP by 16 dB in the $\Theta = 0°$ direction for both planes. In Table 2 comparison of the proposed antenna with the previously reported antenna is listed. LHCP 0° means that at a constant value of $\varphi = 0°$ radiation pattern is dominating in RHCP than left-hand CP and LHCP 90° means that at a constant value of $\varphi = 90°$ radiation pattern is dominating in RHCP than left-hand CP.

Conclusion

A novel structure single-feed triple-band CARMSA has been presented. The proposed antenna depicts a simple structure with compactness and shows RHCP for two bands with linear polarization in one band. Gain of 3.32, 3.54, and 3.83 dBi is achieved in three bands at 1.22760, 1.57542, and 2.18 GHz, respectively. Thus, the proposed antenna finds a good prospective for GPS *L*2, GPS *L*1, and UMTS bands which make this suitable for the automotive applications.

Conflict of interest. None.

References

1. **Baek JG and Hwang KC** (2013) Triple-band unidirectional circularly polarized hexagonal slot antenna with multiple L-shaped slits. *IEEE Transactions on Antennas and Propagation* **61**, 4831–4835.
2. **Kumar A, Deegwal JK and Sharma MM** (2018) Miniaturized wideband dual linearly and circularly polarized printed square slot antenna for multiradio wireless systems. *AEU – International Journal of Electronics and Communications* **88**, 44–51.
3. **Bod M and Hamid Reza H** (2014) Multi-band circularly polarized slot antenna for GPS, Bluetooth and WIMAX bands. *Progress in Electromagnetics Research C* **49**, 171–178.
4. **Gupta S, Kanaujia BK, Dalela C and Patil S** (2020) Design of circularly polarized antenna using inclined fractal defected ground structure for S-band applications. *Electromagnetics* **40**, 526–540.
5. **Jaiverdhan KA, Sharma MM and Yadav RP** (2019) Dual wideband circular polarized CPW-fed strip and slots loaded compact square slot antenna for wireless and satellite applications. *AEU – International Journal of Electronics and Communications* **108**, 181–188.
6. **Zhangfang H, Wei X, Yuan L, Yinping H and Yongxin Z** (2016) Design of a modified circular-cut multiband fractal antenna. *The Journal of China Universities of Posts and Telecommunications* **23**, 68–75.
7. **Gupta S, Patil S, Dalela C and Kanaujia BK** (2021) Analysis and design of inclined fractal defected ground-based circularly polarized antenna for CA-band applications. *International Journal of Microwave and Wireless Technologies* **13**, 397–406.
8. **Oraizi H and Hedayati S** (2012) Circularly polarized multiband microstrip antenna using the square and Giuseppe Peano fractals. *IEEE Transaction on Antennas and Propagation* **60**, 3466–3470.
9. **El Misilmani HM, Al-Husseini M, Kabalan KY and El-Hajj A** (2014) Compact circularly polarized multiband antennas for RFID applications. *International Journal of Antennas and Propagation* **2014**, 1–10.
10. **Chen H-D and Chen H-T** (2004) A CPW-fed dual-frequency monopole antenna. *IEEE Transaction on Antennas and Propagation* **52**, 978–982.

11. **Chen HM and Wong KL** (1999) On the circular polarization operation of annular-ring microstrip antennas. *IEEE Transaction on Antennas and Propagation* **47**, 1289–1292.

12. **Hong YP, Kim JM, Jeong SC, Kim DH and Yook JG** (2005) Low profile S-band dual-polarized antenna for SDARS application. *IEEE Antennas and Wireless Propagation* **4**, 475–477.

13. **Kanaujia BK and Vishvakarma BR** (2004) Analysis of Gunn integrated annular ring microstrip antenna. *IEEE Transactions on Antennas and Propagation* **52**, 88–97.

14. **Ahmed MF, Shaalan A-H and Awadalla HK** (2015) Design and simulation of a single fed multi-band circularly polarized microstrip antenna with slots. *Progress in Electromagnetics Research c* **57**, 71–79.

15. **Kim SM, Yoon KS and Yang WG** (2007) Dual-band circular polarization square patch antenna for GPS and DMB. *Microwave and Optical Technology Letters* **49**, 2925–2926.

16. **Chang TN and Han YL** (2011) Dual-band circularly polarized antenna using combined C-shaped and L-shaped slots excited by a microstrip line. *Microwave and Optical Technology Letters* **53**, 1041–1044.

17. **Nasimuddin N, Chen ZN and Qing X** (2010) Dual-band circularly polarized S-shaped slotted patch antenna with a small frequency-ratio. *IEEE Transaction on Antennas and Propagation* **58**, 2112–2115.

18. **Jou CF, Wu JW and Wang CJ** (2009) Novel broadband monopole antennas with dual-band circular polarization. *IEEE Transactions on Antennas and Propagation* **57**, 1027–1034.

19. **Yu A, Yang F and Elsherbeni A** (2008) A dual band circularly polarized ring antenna based on composite right and left handed metamaterials. *Progress in Electromagnetics Research* **78**, 73–81.

20. **Patil S, Verma A, Kumar Singh A, Kanaujia B and Kumar S** (2021) A low-profile circularly polarized microstrip antenna using elliptical electromagnetic band gap structure. *International Journal of Microwave and Wireless Technologies*, 1–10.

21. **Jung YK and Lee B** (2012) Dual-band circularly polarized microstrip RFID reader antenna using metamaterial branch-line coupler. *IEEE Transaction on Antennas and Propagation* **60**, 786–791.

22. **Pozar DM and Duffy SM** (1997) A dual-band circularly polarized aperture-coupled stacked microstrip antenna for global positioning satellite. *IEEE Transaction on Antennas and Propagation* **45**, 1618–1625.

23. **Falade OP, Rehman MU, Gao Y, Chen X and Parini CG** (2012) Single feed stacked patch circular polarized antenna for triple band GPS receivers. *IEEE Transactions on Antennas and Propagation* **60**, 4479–4484.

24. **Zhou Y, Chen CC and Volakis JL** (2007) Dual band proximity-fed stacked patch antenna for tri-band GPS applications. *IEEE Transaction on Antennas and Propagation* **55**, 220–223.

25. **Patil S, Singh A, Kanaujia B and Yadava R** (2019) A low-profile triple-band circularly polarized wide slot antenna for wireless systems. *International Journal of Microwave and Wireless Technologies* **11**, 67–75.

26. **Patil S, Singh AK, Kanaujia BK and Yadava RL** (2019) A compact, dual wide-band circularly polarized, modified square ring slot antenna for C and Ku band applications. *International Journal of Microwave and Wireless Technologies* **11**, 182–189.

27. **Sun X, Zhang Z and Feng Z** (2011) Dual-band circularly polarized stacked annular ring patch antenna for GPS application. *IEEE Antennas and Wireless Propagation Letters* **10**, 49–52.

28. **Rao BR, Smolinski MA, Quach CC and Rosario EN** (2003) Triple band GPS trap-loaded inverted L antenna array. *Microwave and Optical Technology Letters* **38**, 35–37.

29. **Bao XL and Ammann MJ** (2007) Dual-frequency circularly-polarized patch antenna with compact size and small frequency ratio. *IEEE Transactions on Antennas and Propagation* **55**, 2104–2107.

30. **Choudhary SD, Srivastava A and Kumar M** (2020) Design of single-fed dual-polarized dual-band slotted patch antenna for GPS and SDARS applications. *Microwave and Optical Technology Letters* **63**, 353–360.

31. **Ramirez M, Parron J, Gonzalez-Arbesu JM and Gemio J** (2011) Concentric annular-ring microstrip antenna with circular polarization. *IEEE Antennas and Wireless Propagation Letters* **10**, 517–519.

32. **Wang-Ta H, Tze-Hsuan C and Jean-Fu K** (2012) Dual-band circularly polarized cavity-backed annular slot antenna for GPS receiver. *IEEE Transactions on Antennas and Propagation* **60**, 2076–2080.

33. **Bilgic MM and Yegin K** (2016) Modified annular ring antenna for GPS and SDARS automotive applications. *IEEE Antennas and Wireless Propagation Letters* **15**, 1442–1445.

34. **Ting W, Hao B and Xi-Zheng K** (2017) A compact triple-band antenna with dual-polarization characteristics. *Progress in Electromagnetics Research Letters* **68**, 135–141.

35. **Raheja DK, Kanaujia BK and Kumar S** (2018) A dual polarized triple band stacked elliptical microstrip patch antenna for WLAN applications. *Wireless Personal Communications* **100**, 1585–1599.

36. **Kunwar A, Gautam AK and Rambabu K** (2017) Design of a compact U-shaped slot triple band antenna for WLAN/WiMAX applications. *AEU – International Journal of Electronics and Communications* **71**, 82–88.

37. **Kanaujia BK and Vishvakarma BR** (2003) Analysis of two-concentric annular ring microstrip antenna. *Microwave Opt Technol Lett* **36**, 104–108.

38. **Singh AK, Gangwar RK and Kanaujia BK** (2016) Circularly polarized annular ring microstrip antenna for high gain application. *Electromagnetics* **36**, 379–391.

Surya Deo Choudhary received his Ph.D. degree in Electronics and Communication Engineering from B.R. Ambedkar Bihar University in 2014, his Master of Technology Degree from BIT Sindri, Dhanbad under Vinoba Bhave University in 2011, and his Bachelor (B.Sc. Engineering) in 2008 from the same University. Presently, he is working as an Associate Professor and Deputy Head of Electronics and Communication Engineering Department, Noida Institute of Engineering and Technology, Greater Noida, India. He has wide teaching experience as an Assistant Professor in the Department of ECE, DAV Institute of Engineering & Technology (A joint venture of the Government of Jharkhand & DAVCMC). He has more than 10 years of teaching and research experience. His research interests include organic semiconductor materials, antenna and microwave engineering. He has published many national and international journals. He is a Life Member of the International Association of Engineers (IAENG) and the Indian Society for Technical Education (ISTE).

Shilpee Patil received her Ph.D. degree in Electronics Engineering from AKTU, Lucknow, India in 2019, her Master of Technology degree in Digital Communication from GGSIP University, Delhi, India, in 2009. She received her B.Tech. degree in Electronics & Communication Engineering from AKTU, Lucknow, India. Shilpee Patil currently is working as an Associate Professor in the Department of Electronics & Communication Engineering in NIET, Greater Noida, India. She has more than 11 years of teaching and research experience. She has a keen research interest in design and modeling of microstrip antenna for wireless communications. She has published many national and international journals. She has attended various training programs in the area of Electronics & Communication Engineering. She is a reviewer of several journals of international repute, i.e. *IEEE Access*, *Journal of Electromagnetic Wave and Application*, *International Journal of Electronics*, etc.

Alka Verma received her B.E. degree in Electrical & Electronics from Bangalore University, Karnataka, India. She has completed her M.Tech. degree in Electronics Engineering from Dr. A.P.J Abdul Kalam Technical University (formerly UPTU), Lucknow (U.P.), India and currently pursuing her Ph.D. degree from the same. Her areas of interest are microstrip antennas, electromagnetic band gap structures, and circularly polarized microstrip antennas for wireless communications.

Md Irshad Alam has received his Ph.D. degree in Electrical Engineering from B.R. Ambedkar Bihar University in 2014, his Master of Technology Degree from BIT Sindri, Dhanbad under Vinoba Bhave University in 2011, and his B.Tech. from MIT, Muzaffarpur. Presently he is working as an Assistant Professor of Electrical Engineering Department, Sitamarhi Institute of Technology, Sitamarhi, Bihar, India. His research interests include power system, control system, and organic semiconductor materials.

Vinod M. Kapse is working as a Professor and Director at Noida Institute of Engineering & Technology, Greater Noida since March 2019. He obtained his Bachelor's Degree in Industrial Electronics from Amaravati University, Amaravati, and M.Tech. in Electronics Engineering from Nagpur University, Nagpur. He has done his Ph.D. degree in Electronics Engineering in 2014 from Jabalpur Engineering College, RGPV University, Bhopal. He had started his career in Industry as a VLSI Design Engineer with Sibar Software Services Pvt. Ltd., Hyderabad. He has started his teaching career at Guru Ramdas Khalsa Institute of Science Technology, Jabalpur in 2002 as a lecturer. Later in 2002, he joined Gyan Ganga Institute of Technology & Sciences, Jabalpur and worked as HOD & Professor in the ECE Department and Principal of the Institute. His research areas comprise VLSI design, digital system design and robotics, etc. He has published more than 50 research papers in international/national journals.

Prof. Binod Kumar Kanaujia is working as a Professor in the School of Computational and Integrative Sciences, Jawaharlal Nehru University, New Delhi since August 2016. Dr. Kanaujia had completed his B.Tech. in Electronics Engineering from KNIT, Sultanpur, India in 1994. He did his M.Tech. and Ph.D. degrees in 1998 and 2004, respectively, from the Department of Electronics Engineering, I.I.T. B.H.U., Varanasi, India. He has a keen research interest in design and modeling of reconfigurable circular polarized antenna. He has been credited to publish more than 150 research papers. He is a reviewer of several journals of international repute, i.e. *IET Microwaves, Antennas & Propagation*, *IEEE Antennas and Wireless Propagation Letters*, *Wireless Personal Communications*, *Journal of Electromagnetic Wave and Application*, *Indian Journal of Radio and Space Physics*, *IETE Technical Review*, *International Journal of Electronics*, *International Journal of Engineering Science*, *IEEE Transactions on Antennas and Propagation*, *International Journal of Microwave and Wireless Technologies*, etc.